

# Gas-Phase Pyrolyses of Alkyl Azides:<sup>1-4</sup> Experimental Evidence for Chemical Activation

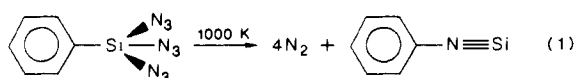
Hans Bock\* and Ralph Dammell<sup>3</sup>

Contribution from the Department of Chemistry, J. W. Goethe University,

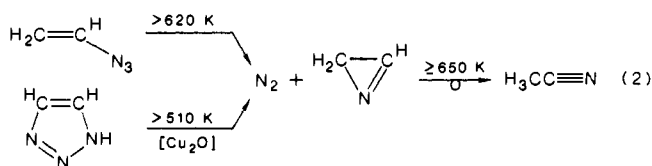
D-6000 Frankfurt/Main 50, Niederurseler Hang, West Germany. Received August 5, 1987

**Abstract:** The thermal decomposition of alkyl azides  $R_3CN_3$  with  $R = H, CH_3,$  or  $HC=CH_2$  has been investigated in a low-pressure flow reactor over the temperature range from 300 to 1200 K by PE spectroscopic real-time gas analysis. The ionization patterns of the azide starting compounds are assigned via Koopmans' theorem on the basis of MNDO calculations, and their recorded changes allow us to determine the  $N_2$  split-off temperatures and to identify the resulting imines  $R_2C=NR$  or other products. Both experimental results and MNDO hypersurface or gradient norm calculations suggest that synchronous nitrogen extrusion and 1,2 R shift from carbon to nitrogen is the energetically most favorable reaction pathway. "Chemical activation" of the intermediate imines  $RHC=NH$ , which cannot dissipate their excess energy under unimolecular conditions, is proven by the temperature dependence of their dehydrogenation to nitriles  $RCN$  in a second reaction channel: e.g.  $H_2C=NH$ , if generated thermally from gaseous  $H_3CN_3$ , splits into  $HCN + H_2$  already at 770 K, whereas if it is prepared by dehydrochlorination of  $H_3CNHCl$ , cool-trapped, and reevaporated, the reaction requires 1300 K.

Thermal decomposition of covalent azides in the gas phase<sup>2-5</sup> at low pressure is attractive for various reasons: Extrusion of the singlet  $N_2$  molecule as a thermodynamically favorable leaving moiety under the (nearly) unimolecular conditions frequently leads to uniform, well-defined reaction channels.<sup>2-4</sup> Thus, when we use a suitable flow reactor to avoid explosions,<sup>6</sup> azide pyrolysis allows us to advantageously generate novel short-lived molecules like phenyl silaisocyanide the first organosilicon compound containing triply bonded, singly coordinated silicon<sup>7</sup> (eq 1). Often the



intermediate can be isolated on a preparative scale, e.g. 2H-azirine<sup>6,8,9</sup> (eq 2). Some of the reactive intermediates, like 2H-



azirine (eq 2), rearrange at higher temperature via an intramolecular 1,2-shift to thermodynamically more stable isomers like nitriles. For this reason azide decomposition also provides an intriguing quantum chemical testing ground for hypersurface calculations.<sup>2-4,6,8,10-12</sup>

(1) Gas-Phase Reactions. 68. Part 66: Reference 2.

(2) For a summary on gas-phase pyrolyses of azides, cf.: Bock, H.; Dammell, R. *Angew. Chem.* **1987**, *99*, 518; *Angew. Chem., Int. Ed. Engl.* **1987**, *26*, 489, and literature cited.

(3) Dammell, R. Ph.D. Thesis, University of Frankfurt, 1986. Present address: Hoechst AG Corporate Research, P.O. Box 800320, D-6230 Frankfurt/Main 50, FRG.

(4) For a preliminary report on the photoelectron spectroscopically optimized pyrolysis of methyl azide, cf.: Bock, H.; Dammell, R.; Horner, L. *Chem. Ber.* **1981**, *114*, 220.

(5) For reviews, cf. e.g.: (a) Bertrand, G.; Majoral, J.-P.; Baccardo, A. *Acc. Chem. Res.* **1986**, *19*, 17. (b) *Azides and Nitrenes*; Scriven, E. F. V., Ed.; Academic: New York, 1984. (c) Brown, R. F. C. *Pyrolytic Methods in Organic Chemistry*; Academic: New York, 1980. (d) L'abbé, G. *Angew. Chem.* **1975**, *23*, 831; *Angew. Chem., Int. Ed. Engl.* **1975**, *14*, 775. (e) *The Chemistry of the Azido Group*; Patai, S., Ed.; Interscience: London, 1971. (f) *Nitrenes*; Lwowski, W., Ed.; Interscience: New York, 1970.

(6) Cf. the review: Bock, H.; Solouki, B. *Angew. Chem.* **1981**, *93*, 425; *Angew. Chem., Int. Ed. Engl.* **1981**, *20*, 427, and literature cited therein. (7) Bock, H.; Dammell, R. *Angew. Chem.* **1985**, *97*, 128; *Angew. Chem., Int. Ed. Engl.* **1985**, *24*, 111. For the 4K matrix isolation, cf.: Gross, G.; Michl, J. *Chem. Eng. News* **1985**, (12) (March 25).

(8) Bock, H.; Dammell, R.; Aygen, S. *J. Am. Chem. Soc.* **1983**, *105*, 7681. Cf. also: Guillemin, J.-C.; Denis, J.-M.; Lasne, M. C.; Ripoll, J.-L. *J. Chem. Soc., Chem. Commun.* **1983**, 238.

Among the analytical methods suited to study potentially explosive compounds such as covalent azides<sup>2-4,7,8,13-15</sup> or  $S_4N_4$ <sup>16</sup> in gaseous flow systems under reduced pressure, photoelectron spectroscopy offers distinct advantages.<sup>6</sup> Only millimole quantities of dangerous compounds need be handled at pressures below 1 Pa; i.e., under (nearly) unimolecular conditions, the temperature dependence over a 300 to 1300 K range can be determined within hours in a single experiment, and the products are readily identified and characterized by their ionization patterns, which via Koopmans' theorem,  $IE_n^v = -\epsilon_j^{SCF}$ , may be correlated with quantum chemical calculations. In contrast to previous thermal decompositions of alkyl azides, carried out with few exceptions<sup>17-20</sup> in condensed phase<sup>5b-f</sup> and usually yielding multicomponent product mixtures, their PE spectroscopically monitored<sup>2-4,6</sup> gas-phase pyrolyses provide information on short-lived intermediates in the respective reaction channels. For example, the  $N_2$  split-off from methyl azide (Figure 1) starts only above a remarkable 720 K(!) and yields the interstellar<sup>21</sup> molecule methanimine,<sup>2-4,22-24</sup> which can be unequivocally identified by its ionization pattern<sup>2-4,25</sup> (eq

(9) Winnewisser, M.; Vogt, J.; Ahlbrecht, H. *J. Chem. Res., Synop.* **1978**, 289. For substituted triazoles, which may react as open-chain azide isomers, see: Gilchrist, T. L.; Gymer, G. E.; Rees, C. W. *J. Chem. Soc., Perkin Trans. 1* **1975**, *8*, and literature cited therein.

(10) Semiempirical hypersurface calculations by the Frankfurt PES group have been summarized by: Bock, H.; Dammell, R.; Roth, B. In *Rings, Clusters and Polymers of the Main Group Elements*; Cowley, A., Ed.; ACS Symposium Series 232; American Chemical Society: Washington, DC, 1983; pp 139-165.

(11) Since our first report on the vinyl azide pyrolysis,<sup>6,8</sup> ab initio calculations on a double- $\zeta$  basis level have been performed, which favor methyl isocyanide as an additional intermediate: Lohr, L. L., Jr.; Hanamura, M.; Morokuma, K. *J. Am. Chem. Soc.* **1983**, *105*, 5541. The PE spectra continuously recorded over the temperature range 300-1000 K, however, do not provide any experimental evidence for its presence in the pyrolysis mixture. Cf. also: Ford, R. G. *J. Am. Chem. Soc.* **1977**, *99*, 2389.

(12) Schaefer, H. F., III *Acc. Chem. Res.* **1979**, *12*, 288. For methyl-nitrene, see also: Yarkony, D. R.; Schaefer, H. F., III; Rothenberg, S. *J. Am. Chem. Soc.* **1974**, *96*, 5974. Demuyneck, J.; Fox, D. J.; Yamaguchi, Y.; Schaefer, H. F., III *Ibid.* **1980**, *102*, 6204.

(13) Bock, H.; Dammell, R. *Inorg. Chem.* **1985**, *24*, 4427.

(14) Bock, H.; Dammell, R. *Z. Naturforsch., B: Anorg. Chem., Org. Chem.* **1987**, *42B*, 301.

(15) Bock, H.; Dammell, R.; Des Marteau, D. D. *Z. Naturforsch., B: Anorg. Chem., Org. Chem.* **1987**, *42B*, 308.

(16) Bock, H.; Solouki, B.; Roesky, H. W. *Inorg. Chem.* **1985**, *25*, 4425.

(17) Rice, F. O.; Grelicki, C. J. *Phys. Chem.* **1957**, *61*, 830.

(18) Brown, R. D.; Godfrey, P. D.; Winkler, D. A. *Aust. J. Chem.* **1980**, *33*, 1.

(19) Geiseler, G.; König, W. Z. *Phys. Chem.* **1964**, *227*, 81. Cf. also: Leermakers, J. A. *J. Am. Chem. Soc.* **1933**, *55*, 2719.

(20) Dunkin, I. R.; Thomson, P. C. P. *Tetrahedron Lett.* **1980**, *21*, 3813. Abramovitch, R. A.; Kyba, E. P. *J. Am. Chem. Soc.* **1974**, *96*, 480.

(21) Cf.: Godfrey, P. D.; Brown, R. D.; Robinson, B. J.; Sinclair, M. *Astrophys. Lett.* **1973**, *13*, 119. Herbst, E. *Astrophys. J.* **1976**, *205*, 94.

(22) Milligan, D. E. *J. Chem. Phys.* **1961**, *35*, 1491.

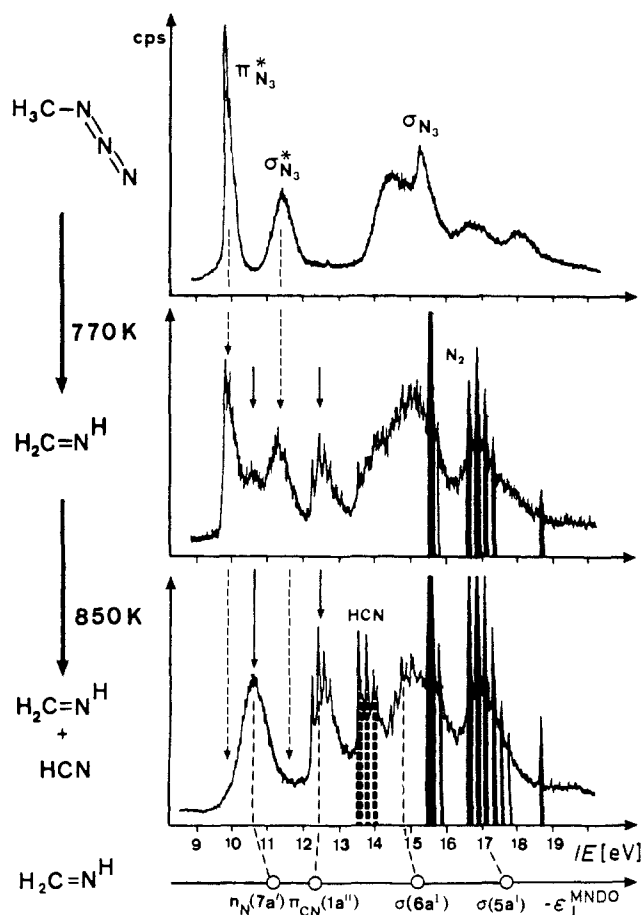
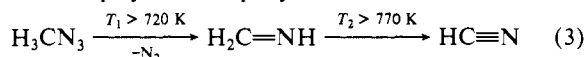


**Figure 1.** He I PE spectrum of methyl azide at 300, 770, and 850 K ( $N_2$ , black; HCN, hatched) and Koopmans' correlation with MNDO eigenvalues for  $H_2C=NH$  (cf. text).

3). In liquid phase, most imines  $R_2C=NR$  ( $R$  or  $R' = H$ ) of small molecular size polymerize rapidly.<sup>26</sup>



As concerns the reaction path of the  $H_3CN_3$  pyrolysis, corroborating preliminary MNDO calculations<sup>3,4</sup> are in accordance with both the high activation barrier for the nitrogen extrusion and the methanimine formation as deduced from the rather large energy calculated for a  $H_3CN\cdots N_2$  saddle point and the shallow minimum for the hypothetical nitrene  $H_3CN$ , which rearranges to  $H_2C=NH$  on a nearly repulsive hypersurface slope.<sup>2-4</sup> In the literature,<sup>5</sup> mechanistic rationalization of alkyl azide decomposition often starts by assuming a nitrene intermediate  $R_3CN$ . According to both ESR measurements<sup>27</sup> and quantum chemical calculations,<sup>5,12</sup> however, nitrenes have a triplet ground state, whereas nonsensitized azide photolysis due to spin conservation yields the excited singlet.<sup>5,28</sup> An "intersystem crossing" in the extremely

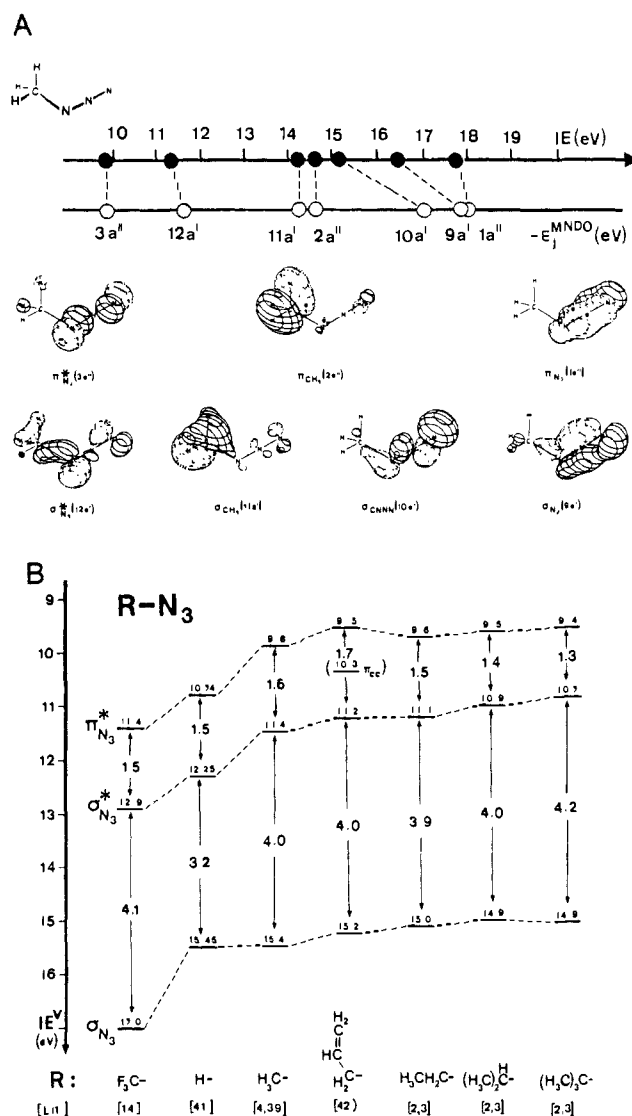


**Figure 2.** Ionization patterns of alkyl azides: (A) Koopmans' assignment for methyl azide based on MNDO calculation and (B) correlation diagram for characteristic  $RN_3$  radical-cation states  $\pi_{N_3}^*$ ,  $\sigma_{N_3}^*$ , and  $\sigma_{N_3}$  (see text).

fast reaction of the rather short-lived singlet nitrenes<sup>5b,f</sup> can only be observed under special measurement conditions, e.g. in inert-gas matrix at 4 K.<sup>23</sup>

Here, we report on the pyrolysis of ethyl, isopropyl, *tert*-butyl, and allyl azides under identical conditions. As concerns the  $N_2$  split off, evidence is provided for preferred synchronous 1,2-shifts to the corresponding imines. In addition, experimental proof for chemical activation of imines produced by thermal decomposition of azides will be presented with the parent compound  $H_3CN_3$  as a transparent example and serves to discuss the formation of nitriles in the consecutive reaction channel.<sup>2-4,8,13-15</sup>

## Experimental Section

**Methyl and Ethyl Azides.**<sup>29</sup> To an aqueous 10%  $NaN_3$  solution in a three-necked flask equipped with two dropping funnels and a Criegee distillation apparatus containing a 265 K cooling finger is added the stoichiometric amount of dialkyl sulfate (only one R group reacts) together with aqueous 5% KOH at a temperature of 350 K. To avoid evolution of dangerous  $HN_3$ , pH 8 has to be controlled continuously by adding an acid-base indicator. The  $RN_3/H_2O$  mixture distilling over is collected in an ice-cooled flask, the layers are separated in a cooled funnel, and the respective  $RN_3$  are dried over  $K_2CO_3$  (to remove traces of  $HN_3$ ) and  $CaCl_2$ . After cautious distillation behind a safety-glass

(29) Grundmann, C. In *Houben-Weyl-Müller Methoden der Organischen Chemie*; Vol X/3, Thieme: Stuttgart, West Germany, 1965; p 782f. and literature cited therein.

(23) Johnson, D. R.; Lovas, F. *J. Chem. Phys.* **1977**, *66*, 4149.

(24) Braillon, B.; Lasne, M. C.; Ripoll, J. L.; Denis, J. M. *Nouv. J. Chim.* **1982**, *6*, 121. Cf. also: Guillemin, J. C.; Denis, J. M. *J. Chem. Soc., Chem. Commun.* **1985**, 951. Guillemin, J. C.; Denis, J. M.; Bogey, M.; Destombes, J. L. *Tetrahedron Lett.* **1986**, *27*, 1147.

(25) (a) Peel, J. B.; Willet, G. *J. Chem. Soc., Faraday Trans. 2* **1975**, *71*, 1799. (b) Frost, D. C.; Lee, S. T.; MacDowell, C. A.; Westwood, N. P. C. *J. Electron Spectrosc. Relat. Phenom.* **1977**, *12*, 95. (c) Schulz, R.; Schweig, A. *Ibid.* **1982**, *28*, 33.

(26) Cf.: *The Chemistry of the C=N Double Bond*; Rappoport, Z., Ed.; Interscience: London, 1970, and literature cited therein.

(27) Wasserman, E.; Smolinski, G.; Yager, W. A. *J. Am. Chem. Soc.* **1964**, *86*, 3166. For methylnitrene, cf.: Wasserman, E. *Prog. Phys. Org. Chem.* **1971**, *8*, 319.

(28) For azide photolysis sensitized by benzoquinone, cf. e.g.: Barash, L.; Wasserman, E.; Yager, W. A. *J. Am. Chem. Soc.* **1967**, *89*, 3921. Lewis, F. D.; Saunders, W. H., Jr. *J. Am. Chem. Soc.* **1968**, *90*, 7033. Pancrazi, A.; Khuong-Huu, Q. *Tetrahedron* **1975**, *31*, 2041.

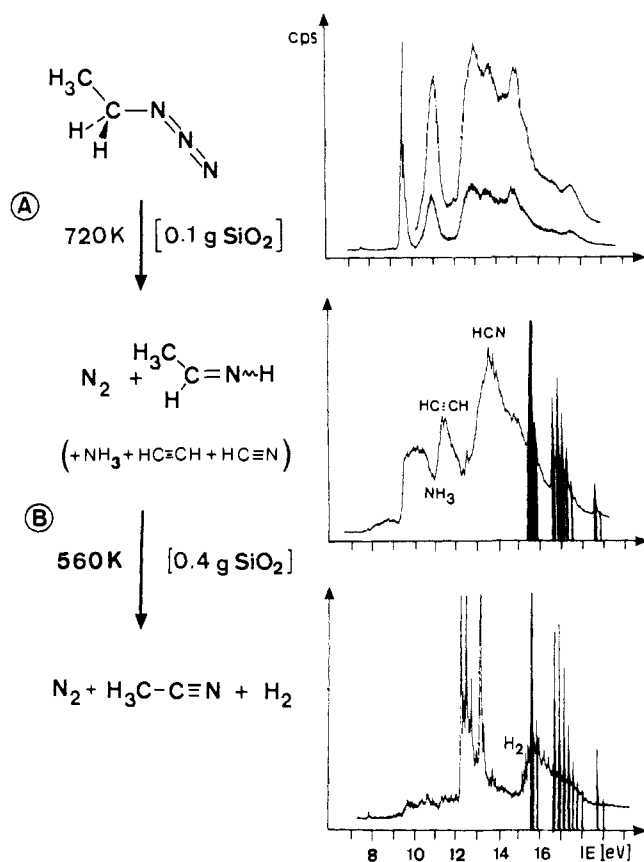


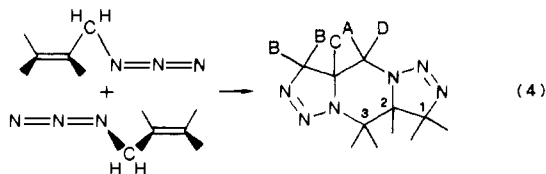
**Figure 3.** He I PE spectra of ethyl azide and during its thermal decomposition under reduced pressure in a heated horizontal reaction tube (eq 5) filled with (A) 0.1 g and (B) 0.4 g of quartz wool ( $N_2$ : black; cf. text).

shield, methyl (bp 291 K) and ethyl (bp 322 K) azides are isolated NMR or PE spectroscopically pure (Figures 1 and 3) in about 70% yield.

**Isopropyl azide**<sup>30</sup> has been prepared under the above precautions from isopropyl bromide and  $NaN_3$  in DMF/ $H_2O$  in 85% yield (bp 350 K) and its purity checked by NMR and PES.

**tert-Butyl Azide.**<sup>31</sup> Under dried nitrogen, 10 g (0.11 mol) of *tert*-butyl chloride, 15 g (0.23 mol) of powdered  $NaN_3$ , and 4 g (0.04 mol) of powdered water-free  $ZnCl_2$  are stirred at room temperature in 100 mL of  $CS_2$ . On addition of 15 mL of DMF, the solution warms up and becomes yellow. After 10 h, the solution is filtered off and distilled, yielding 7.3 g (74%) of *tert*-butyl azide (bp 345 K). Purity is checked by NMR ( $\delta$  1.60 (s,  $CS_2$ )) and PE spectra (Figure 4). The filtered-off yellow solid has to be immediately dissolved in excess water; if a concentrated aqueous solution is allowed to stand in a beaker, explosive whitish crystals of unknown composition form.

**Allyl Azide.**<sup>32a</sup> A total of 10 g of allyl iodide and 4 g of  $NaN_3$  in 75 mL of a 2:1 DMF/ $H_2O$  mixture are heated to reflux for 1 h. After the reflux cooler is replaced with a Criegee distillation apparatus, an azide/water mixture is cautiously distilled off within 2 h. After it is dried over  $CaCl_2$ , fractionate distillation yields 4 g (80%) of allyl azide (bp 345–348 K), the purity of which is checked by its NMR and PE spectra.<sup>42</sup> On standing, crystals (mp 465 K) of composition  $C_6H_{10}N_6$  form (Found: C, 43.44; H, 6.07; N, 50.48. Calcd: C, 43.37; H, 6.01; N, 50.621) for which a 70-eV mass spectrum yields a parent peak  $m/e$  166 as well as  $m/e$  110 ( $M - 2N_2$ ), 83 ( $M/2$ ), 55 (100%) ( $C_3H_5N$ ). The structure of the dimer<sup>32b</sup> (eq 4) is also confirmed by  $^1H$  and  $^{13}C$  NMR.



(30) Olah, G. O.; Donovan, D. J. *J. Org. Chem.* **1978**, *43*, 864.

(31) Miller, J. A. *Tetrahedron Lett.* **1975**, *34*, 2959, and literature cited therein. Cf. ref 20.

(32) (a) Forster, M. O.; Fierz, H. E. *J. Chem. Soc.* **1908**, *93*, 1174. (b) Pezullo, J. C.; Boyko, J. R. *J. Org. Chem.* **1973**, *38*, 168. (c) Reference 42.

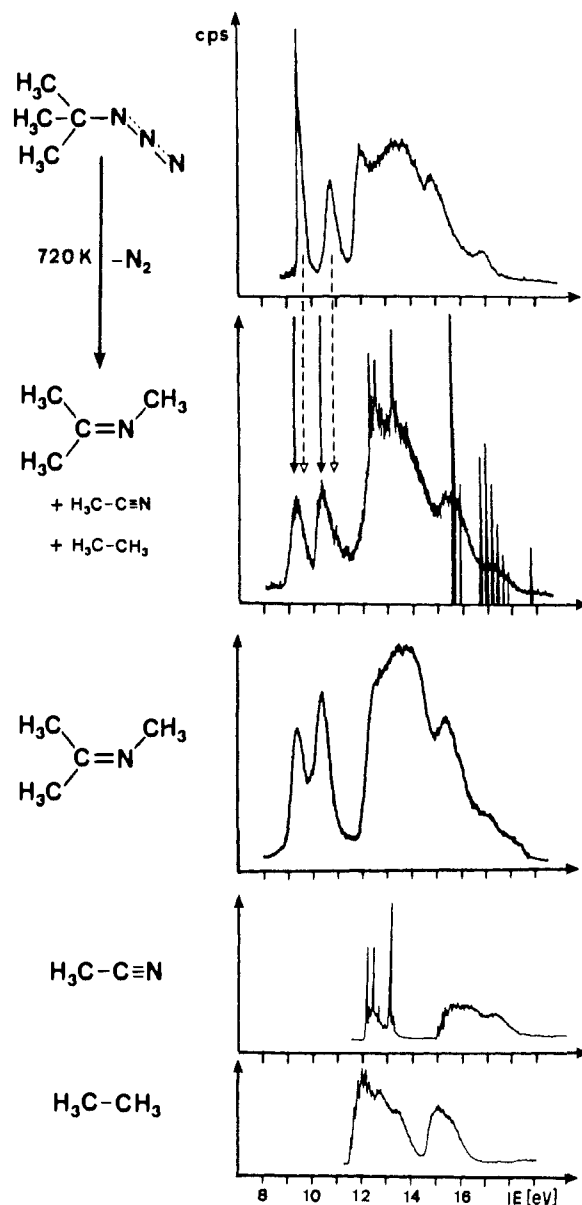


**Figure 4.** He I PE spectra of *tert*-butyl azide, of its 770 K pyrolysis mixture ( $N_2$ : black), and, for comparison, of acetone *N*-methylimine,<sup>33b</sup> acetonitrile, and ethane<sup>43</sup> (see text).

A:  $\delta$  4.19 (2, dd),  $J_{AC} = 4.8$  Hz,  $J_{AD} = 13.5$  Hz. B:  $\delta$  4.05 (4, d),  $J_{BC} = 7.5$  Hz. C:  $\delta$  3.65 (2, tdd),  $J_{DC} = 11.0$  Hz. D:  $\delta$  3.20 Hz (2, dd).  $C_1$ :  $\delta$  68.0 (t).  $C_2$ :  $\delta$  53.8 (d).  $C_3$ :  $\delta$  47.0 (tt).

**Methanimine.**<sup>2-4,33</sup> The gas-phase preparation via chlorination of methylamine over *N*-chlorosuccinimide and subsequent dehydrochlorination of the resulting  $H_3CNHCl$  over potassium *tert*-butylate<sup>33a</sup> has been optimized PE spectroscopically.<sup>33b</sup> The pure compound is co-trapped at 72 K and reevaporated at 160 K; above this temperature rapid polymerization is observed.

**Photoelectron spectra** were recorded on a Leybold-Heraeus spectrometer UPG 200<sup>6</sup> equipped with a molybdenum tube furnace.<sup>34</sup> Throughout the experiments, resolution was about 20 meV; all spectra have been calibrated by the  $N_2$  ( $2^2\Sigma_g^+$ ) and Ar ( $2^2P_{3/2}$ ) peaks at 15.60 and 15.76 eV, respectively.

(33) (a) Braillon, B.; Lasne, M. C.; Ripoll, J. L.; Denis, J. M. *Nouv. J. Chim.* **1982**, *6*, 121. Guillemin, J. C.; Denis, J. M. *Angew. Chem.* **1982**, *94*, 715; *Angew. Chem., Int. Ed. Engl.* **1982**, *21*, 690; *Angew. Chem. Suppl.* **1982**, 1515 f. (b) Bock, H.; Dammel, R. *Chem. Ber.* **1987**, *120*, 1961, 1971. Cf. also: Bock, H.; Solouki, B.; Aygen, S.; Brähler, G.; Dammel, R.; Giordan, J.; Hänel, P.; Herrmann, H.; Hierholzer, B.; Hirabayashi, T.; Jaculi, D.; Kaim, W.; Lechner-Knoblach, U.; Mohmand, S.; Müller, H.; Rittmeyer, P.; Roth, B.; Stein, U. *Nova Acta Leopold.* **1985**, *264/59*, 101.

(34) Cf.: Solouki, B.; Bock, H.; Appel, R.; Westerhaus, A.; Becker, G.; Uhl, G. *Chem. Ber.* **1982**, *115*, 3748.

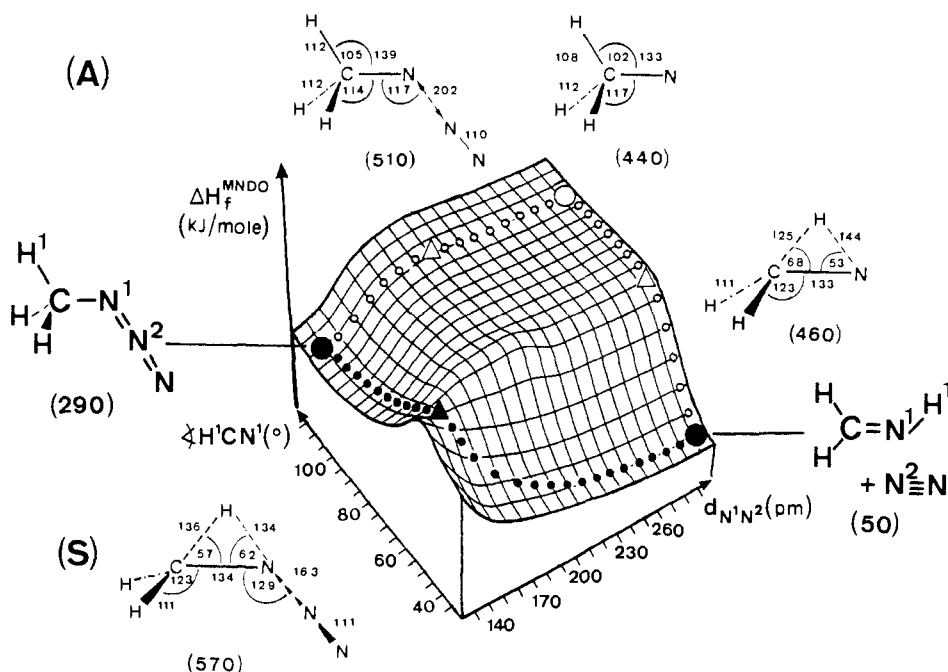
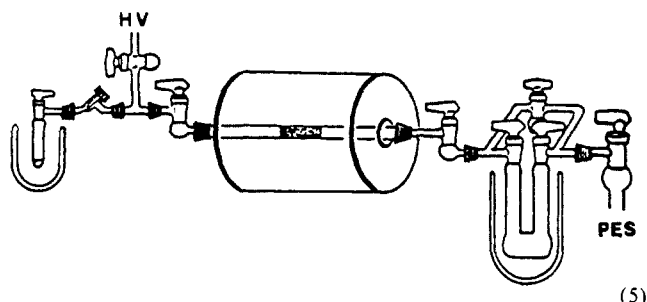


**Figure 5.** MNDO energy hypersurface for  $N_2N$  extrusion and 1,2  $H^1$  shift during the thermal decomposition of methyl azide to methanimine: (A) asynchronous pathway via methylnitrene ( $\Delta O \Delta \Rightarrow$ ) and (S) synchronous movement of  $N_2N$  and  $H^1$  ( $\bullet \blacktriangle \Rightarrow$ ). For details, e.g. concerning the saddle points ( $\Delta$ ,  $\blacktriangle$ ) and their calculated enthalpies of formation ( $\Delta H_f^{MNDO}$ , in parentheses) see text.

Gas-phase pyrolyses were carried out in a quartz tube (length 35 cm, diameter 1.5 cm) heated in a temperature-controlled oven over 30-cm length<sup>6</sup> (eq 5). The azides  $RN_3$  are evaporated from the evacuated (HV)



storage vessel connected via a Teflon precision valve. In the building-block apparatus (eq 5), an additional cooling trap for isolation of pyrolysis products is inserted between reaction tube and PE spectrometer PES, which can be bypassed during optimization of the pyrolysis conditions.

The reaction pressure, as measured at the entrance to the flow reactor, amounts to 0.025 mbar and is kept constant to within  $\pm 0.05$  mbar for all experiments. For the reactor geometry, the pyrolysis temperatures, and the pressures used, the gas passes the system close to the limit for a Knudsen molecular flow<sup>35a</sup> ( $1 < K_n < 3$ ), with the Knudsen number  $K_n$  also approximating the ratio between wall and two body collisions. According to the standard formula for Knudsen conditions,<sup>35b</sup> average residence times between 30 and 50 ms are estimated.

The onset of decomposition is detected by the appearance of the unequivocally recognizable  $N_2$  ( $2\Sigma_g^+$ ) ionization at 15.60 eV, and since the photoionization cross section of  $N_2$  considerably exceeds that of organic molecules in this region,<sup>43</sup> conversions of even a few percent are easily observed. Complete decomposition can be monitored by the disappearance of the prominent azide  $\pi_{N_3}^*$  band. Temperatures thus determined were reproducible to within  $\pm 10$  K. Consistent with the arguments on chemical activation of imine intermediates, the yield of methanimine increases relative to that of HCN if methyl azide is pyrolyzed at higher total pressure of, e.g., 0.06 mbar (cf. the spectrum in Figure 1). Since

the residence time is approximately pressure independent within the Knudsen limit, both starting and end-point temperatures of the decomposition are unaffected by small changes in pressure.

Altogether, preparation and pyrolyses of numerous covalent azides  $RN_3$  have been carried out<sup>2,3</sup> without ever encountering any explosion<sup>5</sup> or poisoning.<sup>5</sup> Nevertheless, due to the most dangerous bulk properties of liquid or solid azides  $RN_3$ , every precaution imaginable (safety-glass shield, fencing mask, leather gloves, deactivation of scratched glass surfaces by refluxing with a  $R_3SiCl/R_2SiCl_2$  mixture, etc.)<sup>2,3</sup> is strongly recommended.

MNDO calculations have been performed at our VAX 11/750 computer with the MOPAC program package provided by M. J. S. Dewar.<sup>36</sup> Full-geometry optimization was carried out for all compounds. Hypersurfaces were calculated by assigning fixed values to the appropriate coordinates and optimizing all others. The distance between grid points was 5–10° for the angle-dependent hypersurfaces. Checks were made by calculating reaction pathways from different starting points. Results were consistent to within  $\pm 1$  kJ/mol. For saddle-point determinations, the systematic location procedure in the SPLOC or MOPAC programs<sup>37</sup> has been used, and the resulting approximate transition-state geometries were refined by gradient norm minimization. In all cases, diagonalization of the Hessian matrix yielded a single negative eigenvalue. Minimum-energy reaction paths were then determined by stepping down from the saddle point with Müller's algorithm,<sup>37b</sup> which, although gradient following, does not require explicit knowledge of gradients: Starting at the saddle point, energy minimization on a hemihypersphere yields a path point  $P_n$ , which in turn serves as the center for the hypersphere yielding  $P_{n+1}$ ; the reaction path is thus approximated to any desired exactitude by a series of equidistant path points.<sup>37b</sup> A graphical representation of the reaction path may be obtained by plotting all path-point geometries into one figure: in Figure 6, a hypersphere radius of  $1/10$  the distance from saddle point to minimum was used. The reaction coordinate is then defined as the sum of all path segment lengths from the minimum to the path point and is often normalized to the sum of all path segment lengths from minimum to minimum.

#### Ionization Patterns of Alkyl Azides $RN_3$

Thermal decomposition of azides in the gas phase is conveniently monitored by the characteristic ionization patterns of  $RN_3$  precursors and of  $N_2$  as well as of other products (Figures 1, 3, and 4), which are continually recorded by the attached PE spec-

(35) (a) Cf. e.g.: Dushman, S.; Lafferty, J. M. *Scientific Foundations of Vacuum Techniques*; Wiley: New York, 1962. Roth, A. *Vacuum Technology*; North-Holland: Amsterdam, The Netherlands, 1976. Mulcahy, M. F. R. *Gas Kinetics*; Nelson: London, 1973. (b) Cf.: Golden, D. M.; Spokes, G. N.; Benson, S. W. *Angew. Chem., Int. Ed. Engl.* 1973, 12, 534. Seybold, G. *Angew. Chem., Int. Ed. Engl.* 1977, 16, 365. The review by: Brown, R. F. C. *Pyrolytic Methods in Organic Chemistry*; Academic: New York, 1980.

(36) Dewar, M. J. S.; Thiel, W. *J. Am. Chem. Soc.* 1977, 99, 4907.

(37) (a) Roth, B. Ph.D. Thesis, University of Frankfurt, 1983. (b) Müller, K. *Angew. Chem.* 1980, 92, 1; *Angew. Chem., Int. Ed. Engl.* 1980, 19, 1, and literature cited therein. E.g.: Müller, K.; Brown, L. D. *Theor. Chim. Acta* 1979, 53, 75.

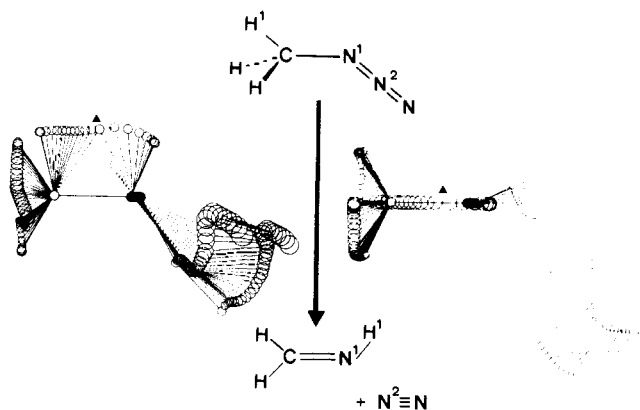


**Figure 6.** Stroboscopic representation of MNDO-calculated geometry changes along the reaction coordinate for methyl azide decomposition with synchronous  $N_2$  extrusion and 1,2 H shift viewed both perpendicular to and in the CNNN plane ( $\blacktriangle$ : transition state (Figure 5); see text).

trometer (eq 5). Since no restrictive selection rules exist for photoionization in contrast to, e.g., vibrational spectroscopy, all molecules leaving the heated zone in concentrations greater than ca. 5% may be identified from their unmistakable ionization "fingerprints". In particular, the "azide leaving group"  $N_2$  can be unequivocally identified by the appearance of its needlelike bands above 15.5 eV (Figures 1, 3, and 4; black), and, therefore, their appearance allows us to determine the decomposition temperature of the respective azide  $RN_3$  within the heated flow system.<sup>2-4,8,13-15</sup> In addition, most covalent azides  $RN_3$  also exhibit three prominent and partly needlelike bands, the disappearance of which signals complete decomposition (Figures 1, 3, and 4;  $\rightarrow$ ).

In general, the energies of "vertical" ionization processes may be correlated in a satisfactory approximation<sup>38,39</sup> using Koopmans' theorem,  $IE_n^v = -\epsilon_j^{SCF}$ , with the SCF eigenvalues calculated for the neutral molecule. With methyl azide as an illustration, its He I PE spectrum (Figure 1) as expected<sup>27</sup> shows seven ionization bands,<sup>4,40</sup> which are assigned via Koopmans' correlation,  $IE_n^v = -\epsilon_j^{MNDO}$  (Figure 2A). Because of the nodes through the CNNN plane and, perpendicularly, through the central nitrogen displayed in the corresponding MNDO orbital diagram (Figure 2A), the radical-cation ground state  $\dot{X}(^2A')$  is often in shorthand denoted  $\pi_{N_3}^*$ .<sup>35</sup> Relative to the pertinent needlelike low-energy PE band readily recognized in all alkyl azide ionization patterns (Figures 1, 3, and 4), the two other  $\pi(a')$  states of  $H_3CN_3^+$  at 14.7 and 18 eV with dominant  $H_2C^-$  and  $NNN^-$  contributions appear less prominently in its PE spectrum (Figure 1). More characteristic are the second and fifth bands at 11.4 and 15.4 eV, which are assigned to the first excited radical-cation state  $\dot{A}(^2A)$  and to the  $\dot{D}(^2A)$  state, which, due to their dominant  $NNN$  contributions and perpendicular nodes, are frequently abbreviated  $\sigma_{N_3}^*$  and  $\sigma_{N_3}$ .<sup>5</sup>

Comparing the ionization energies of the three characteristic  $(R)NNN^+$  radical-cation states (Figure 2B) provides information on the effects of substituents  $R$ .<sup>2</sup> Although in each of the  $\pi_{N_3}^*$ ,  $\sigma_{N_3}^*$ , and  $\sigma_{N_3}$  states the positive charge is largely localized in the  $NNN$  subunit (Figure 2A), the energies  $IE_n^v$  exhibit a marked dependence on  $R$ ; e.g., on exchange of  $C(CH_3)_3$  for  $CF_3$ , all three typical ionization energies increase by an equal amount of about 2 eV. This indicates that  $\pi$  and  $\sigma$  perturbations<sup>39</sup> parallel each other, so that acceptor or donor substituent effects may be defined relative to  $R = H$  or  $CH_3$ . As concerns the parent compound  $HN_3$ ,<sup>41</sup> the small difference of only 3.2 eV between  $\sigma_{N_3}^*$  and  $\sigma_{N_3}$

can be rationalized in a simplified manner as being due to lack of interspersed radical-cation states with dominant substituent contributions. For all alkyl azides, characteristic ionizations  $\pi_{N_3}^*$ ,  $\sigma_{N_3}^*$ , and  $\sigma_{N_3}$  are found within narrow regions (Figure 2B), because these predominantly  $NNN^+$  localized states will only be slightly stabilized with increasing size of  $R$  groups. This argument is further supported by the PE spectrum of allyl azide,<sup>42</sup> in which the vinyl and azide groups are isolated from one another by a  $CH_2$  bridge and which shows the additional  $\pi_{CC}$  ionization close to the one of propene (10.03 eV<sup>43</sup>).

Naturally, neither the characteristic radical-cation state patterns of azides  $RN_3$  nor the MO calculations for their assignment allow us to draw any conclusions<sup>5</sup> regarding their thermal stabilities or their decomposition products formed after  $N_2$  elimination. On the other hand, the  $RN_3^+$  state comparison (Figure 2B) can be used to check the assignment of the PE spectra based on the SCF calculations, which for azides  $RN_3$  tend to somewhat larger Koopmans' deviations<sup>44</sup> and thus provide an indispensable prerequisite for monitoring azide gas-phase pyrolyses by means of real-time PE spectroscopic analysis.<sup>6</sup>

### Alkyl Azide Pyrolyses under Reduced Pressure

The thermal decomposition of compounds  $RN_3$  is carried out under (nearly) unimolecular conditions (cf. the Experimental Section) in an externally heated quartz tube, often filled with differing amounts of quartz wool (eq 5). As discussed in the preceding section, the appearance of the  $N_2$  PES spikes allows us to determine the temperature of beginning pyrolysis, and the disappearance of the needlelike  $\pi_{N_3}^*$  bands of the respective alkyl azides, that of completed decomposition.

**Methyl Azide.** Since our preliminary report on the  $H_3CN_3$  pyrolysis,<sup>4</sup> the basic reaction for experimental proof of chemical activation as well as for calculations of microscopic azide decomposition pathways as discussed subsequently, the experiment has been repeated many times.<sup>3</sup> The  $N_2$  split off begins at 720 K; above 770 K the PE bands of methanimine at 10.6 and 12.5 eV become clearly visible, and at 850 K the  $H_3CN_3$  ionization patterns has vanished (Figure 1). The additional new band between 13.6 and 14.2 eV, exhibiting characteristic vibrational fine structure<sup>43</sup> (Figure 1; hatched) proves HCN to be one product of a consecutive decomposition channel. The formation of the interstellar molecule  $H_2C=NH$  as the first detectable intermediate in the  $H_3CN_3$  pyrolysis under reduced pressure<sup>4</sup> has been confirmed in various ways:<sup>3,33</sup> flanging the thermolysis apparatus on a mass spectrometer, the  $H_3CN_3^+$  parent peak at  $m/e$  57 disappears at 870 K, while the intensity of the  $H_3CN^+$  peak at  $m/e$  29 has increased considerably.<sup>3</sup> Methanimine, prepared independently by dehydrochlorination of  $H_3CNHCl$  on solid KOR,<sup>33</sup> cool-trapped, and reevaporated at temperatures below 150 K, yields a PE spectrum, which after electronic subtraction<sup>45</sup> of the  $N_2$  and HCN ionization bands is identical with the one recorded during the 850 K pyrolysis of  $H_3CN_3$ . Furthermore, the  $H_2C=NH$  ionization pattern can be satisfactorily correlated with MNDO eigenvalues (Figure 1), and both energy hypersurface and gradient norm calculations for the  $H_3CN_3$  decomposition pathway of lowest energy (Figure 6) also exclude the formation of a different intermediate.

**Ethyl azide decomposition under reduced pressure**<sup>3,18,19</sup> (Figure 4) shows a marked dependence on the quartz wool filling of the heated tube (eq 5):<sup>3</sup> With 0.1 g of  $SiO_2$ ,  $N_2$  extrusion starts at 660 K and thermolysis is complete above 770 K. A mixture of

(38) Cf. e.g.: Bock, H.; Ramsey, B. G. *Angew. Chem.* **1973**, *85*, 773; *Angew. Chem., Int. Ed. Engl.* **1973**, *12*, 734, and literature cited therein.

(39) Cf. e.g.: Bock, H. *Angew. Chem.* **1977**, *89*, 632; *Angew. Chem., Int. Ed. Engl.* **1977**, *16*, 613, and literature cited therein.

(40) Cf. also: Cradock, S.; Ebsworth, E. A. V.; Murdoch, J. D. *J. Chem. Soc., Faraday Trans.* **1971**, *67*, 86.

(41) (a) Eland, J. H. D. *Philos. Trans. R. Soc. London, A* **1970**, *268*, 87. (b) Reference 39. (c) Lee, T. H.; Colton, R. J.; Rabalais, J. W. *J. Am. Chem. Soc.* **1975**, *97*, 4845. (d) Bastide, J.; Maier, J. P. *Chem. Phys.* **1976**, *12*, 177. (e) Cvitas, T.; Klasinc, L. *J. Chem. Soc., Faraday Trans.* **2** **1976**, *72*, 1240.

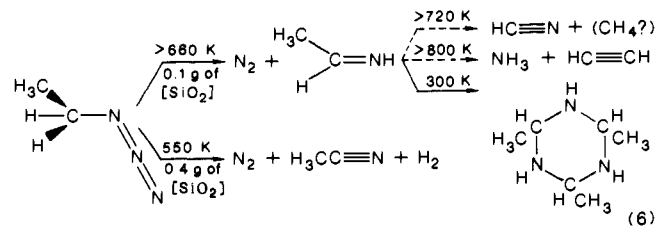
(42) Cf.: Herrmann, W. A.; Kriechbaum, G. W.; Dammel, R.; Bock, H. *J. Organomet. Chem.* **1983**, *254*, 219, and literature cited therein.

(43) Cf. e.g.: *Handbook of He I Photoelectron Spectra*; Kimura, K., Katsumata, S., Achiba, Y., Yamazaki, T., Iwata, S., Eds.; Halsted: New York, 1981.

(44) E.g. for  $IE_3^v = 15.45$  eV of  $HN_3$ ,<sup>41</sup> calculated values deviate up to 18.51 eV although obtained with a double- $\zeta$  basis set: Wyatt, J. F.; Hillier, I. H.; Saunders, V. R.; Connor, J. A.; Barber, M. *J. Chem. Phys.* **1971**, *54*, 5311.

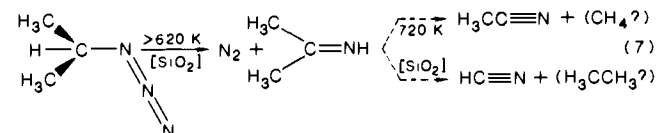
(45) Cf. e.g.: Bock, H.; Solouki, B.; Maier, G. *Angew. Chem.* **1985**, *97*, 205; *Angew. Chem., Int. Ed. Engl.* **1985**, *24*, 205. Binnewies, M.; Solouki, B.; Bock, H.; Becherer, R.; Ahlrichs, R. *Ibid.* **1984**, *96*, 704; **1984**, *23*, 731.

(*Z*)- and (*E*)-ethanimines results as the main product, in addition, low-intensity PE bands of byproducts HCN, NH<sub>3</sub>, and HC≡CH are observed. After reevaporation of the cool-trapped H<sub>3</sub>CH-C≡NH, crystals of trimeric 2,4,6-trimethylhexahydro-*s*-triazine, identified by <sup>1</sup>H NMR, remain behind (eq 6). When the quartz



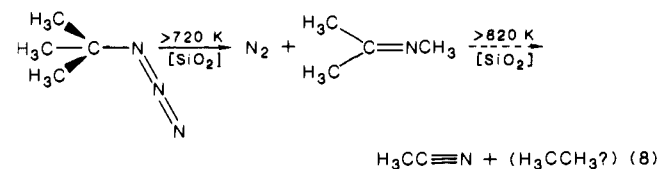
tube is filled with increasing amounts of quartz wool, the decomposition temperature gradually decreases to about 620 K, accompanied by rather small changes in product composition as expected from only slightly increased contact times. If, however, the original amount of quartz wool is exceeded 4 times (6:0.4 g), the decomposition temperature drops abruptly to 550 K and the product spectrum changes completely (Figure 4B): The previously unobserved acetonitrile and H<sub>2</sub> are now the main products. Presumably, this change is due to the reaching of the H<sub>3</sub>C<sub>2</sub>N<sub>3</sub> explosion limit,<sup>19</sup> setting off a thermal chain reaction, which leads to the entropically most favored products.

**Isopropyl azide** begins to decompose above 620 K, with N<sub>2</sub> being completely cleaved at 770 K.<sup>3</sup> The main product, acetone imine, is identified by PE spectroscopic comparison with an independently prepared sample<sup>33</sup> as well as by a satisfactory Koopmans' correlation of its ionization pattern with MNDO eigenvalues. In addition, both acetonitrile and HCN are PE spectroscopically<sup>43</sup> detected as byproducts (eq 7). As in the case of ethyl azide (eq

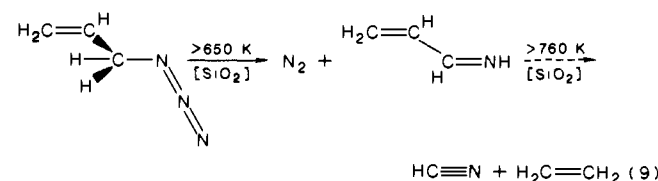


6), the stoichiometrically required decomposition products CH<sub>4</sub> and C<sub>2</sub>H<sub>6</sub> from a "chemically activated" acetone imine cannot be identified with certainty due to their rather contourless PE spectra<sup>43</sup> (cf. Figure 4).

**tert-Butyl azide** requires temperatures of at least 720 K before nitrogen is eliminated.<sup>3</sup> According to the PE spectra recorded (Figure 4), shown here also as an example for the PE spectroscopic analysis of decomposition product mixtures,<sup>6</sup> the main decomposition product is acetone *N*-methylimine, accompanied by acetonitrile and, probably, ethane as byproducts (eq 8). On increase of the oven temperature above 820 K, acetonitrile becomes the main product.



**Allyl azide**, monomeric (cf. the Experimental Section) and planar in the gas-phase,<sup>32,42</sup> decomposes above 600 K into N<sub>2</sub> and acrolein imine, which can be isolated by condensation in a cold trap<sup>3</sup> (eq 9). At oven temperatures above 760 K, a second reaction

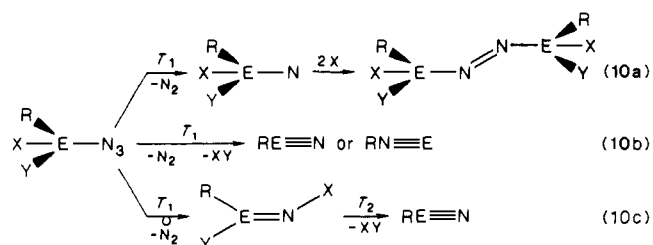


channel to hydrogen cyanide and ethene is opened, presumably via chemical activation of the intermediate acrolein imine.

In summary, the alkyl azides RN<sub>3</sub> studied, with R = CH<sub>3</sub>, CH<sub>3</sub>-*n*(CH<sub>2</sub>)<sub>*n*</sub> (*n* = 1–3), and CH<sub>2</sub>HC=CH<sub>2</sub>, exhibit rather similar thermolysis behavior: N<sub>2</sub> extrusion begins within a relatively narrow temperature range.<sup>2,46</sup> The primary products, methanimines, formed via 1,2 H shifts or via 1,2 R migration have been detected by PE spectroscopic real-time analysis in the flow system and can be isolated by condensation in a cold trap (eq 5). Finally, at temperatures only 50–110 K higher or on prolonged contact time, alkyl azides in addition to N<sub>2</sub> also split off H<sub>2</sub>, alkanes, or alkenes to yield the thermodynamically rather stable end products HCN or H<sub>3</sub>CCN (Figures 1, 3, and 4). The observed small temperature difference between the two consecutive reaction channels in eq 2, 3, and 6–9 suggests that the intermediate methanimines are chemically activated, i.e. cannot efficiently dissipate their internal energy accumulated in the azide pyrolysis under (nearly) unimolecular conditions.<sup>47</sup>

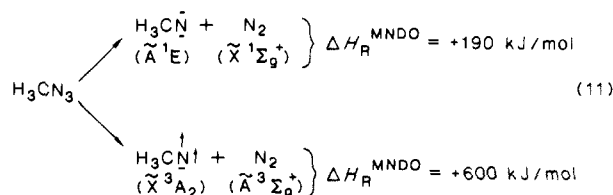
### Discussion of the Alkyl Pyrolysis Path

For the gas-phase pyrolysis of main-group element azides, a variety of thermal decomposition channels have been reported<sup>2,5</sup> (eq 10). Nitrenes in singlet ground states (eq 10a) so far have



been proven only for molecules such as FN, R<sub>2</sub>NN, or R<sub>2</sub>PN,<sup>2,5</sup> and any dimerization to azo compounds (eq 10a) has been observed only at higher pressure.<sup>2,5</sup> From acceptor-substituted azides, usually N<sub>2</sub> is eliminated together with another fragment XY like N<sub>2</sub>,<sup>2,7</sup> HF,<sup>2,13</sup> F<sub>2</sub>,<sup>2,14</sup> or HCl,<sup>2,15</sup> at the same temperature T<sub>1</sub> (eq 10b) to yield nitriles or isonitriles (cf. eq 1) and, therefore, within the PE spectroscopic time resolution of >10<sup>-3</sup> s, no intermediates can be detected. The formation of methanimine derivatives from alkyl azides (eq 10c: E = C and R, X, Y = H, alkyl)<sup>2-4,8</sup> and their decomposition at temperatures T<sub>2</sub> to nitriles reported in the preceding chapter raises numerous questions concerning details of the reaction pathway, which will be discussed subsequently based on the experimental observations and on additional MNDO hypersurface and gradient norm calculations.<sup>2,3</sup>

**Singlet or Triplet Intermediates?** For the parent alkyl azide H<sub>3</sub>CN<sub>3</sub>, the N<sub>2</sub> splitoff under approximately unimolecular conditions has been determined by PE spectroscopy to begin at 720 K. This at first sight surprisingly high temperature, nevertheless, is in agreement with the estimated H<sub>3</sub>CN–N<sub>2</sub> bond dissociation energy of 170 kJ/mol.<sup>5,47</sup> For methylnitrene as a hypothetical dissociation product, double-ζ SCF calculations<sup>12</sup> predict a triplet ground state  $\tilde{X}(^3A_2)$  and higher by 170 kJ/mol (MNDO:<sup>3</sup> 180 kJ/mol) an excited singlet state  $\tilde{A}(^1E)$ . However, spin conservation due to the extremely large energy difference of 590 kJ/mol between the singlet ground state of N<sub>2</sub>, X(<sup>1</sup>Σ<sub>g</sub><sup>+</sup>), and its lowest excited triplet state, A(<sup>3</sup>Σ<sub>u</sub><sup>+</sup>), would require that singlet methylnitrene should be formed preferentially<sup>3</sup> (eq 11). Together



(46) Cf. e.g.: Jones, W. M. In *Rearrangements of Ground and Excited States*; de Mayo, P., Ed.; Academic: New York, 1980; S. 95 ff and literature cited therein. See also ref 5b.

(47) Cf. e.g.: Wentrup, C. *Reactive Molecules*; Wiley-Interscience: New York, 1984; p 162 ff, and literature cited therein.

**Table I.** MNDO Heats of Formation for Methyl, Ethyl, Isopropyl, and *tert*-Butyl Azides, for Saddle Points of Their Synchronous N<sub>2</sub> Extrusion and 1,2 H Shift or 1,2 CH<sub>3</sub> Migration, and for the Resulting Products<sup>a</sup>

1,2 H shift			1,2 CH <sub>3</sub> migration			
azide: $\Delta H_f^{\text{MNDO}}$ , kJ/mol	product: $\Delta H_f^{\text{MNDO}}$ , kJ/mol	saddle point: $\Delta H_f^{\text{MNDO}}$ , kJ/mol	geometry, pm and deg	product: $\Delta H_f^{\text{MNDO}}$ , kJ/mol	saddle point: $\Delta H_f^{\text{MNDO}}$ , kJ/mol	geometry, pm and deg
H <sub>3</sub> CN <sub>3</sub> : 290	H <sub>2</sub> C=NH: 50	570				
H <sub>3</sub> CH <sub>2</sub> CN <sub>3</sub> : 268	H <sub>3</sub> CHC=NH: cis, 42; trans, 41	530		H <sub>2</sub> C=NCH <sub>3</sub> : 72	570	
(H <sub>3</sub> C) <sub>2</sub> HCN <sub>3</sub> : 256	(H <sub>3</sub> C) <sub>2</sub> C=NH: 12	515		H <sub>3</sub> CHC=NCH <sub>3</sub> : cis, 44; trans, 37	535	
(H <sub>3</sub> C) <sub>3</sub> CN <sub>3</sub> : 251				(H <sub>3</sub> C) <sub>2</sub> C=NCH <sub>3</sub> : 1	535	

<sup>a</sup>All saddle point geometries have been gradient norm minimized (see text).

with other experimental observations,<sup>5b,f,23,27,28</sup> the energy estimate (eq 11) suggests that both thermal formation of methylnitrene from H<sub>3</sub>CN<sub>3</sub> and its subsequent reactions should occur on singlet energy hypersurfaces.

**Asynchronous or Synchronous Hydrogen 1,2-Shift?** The two principal pathways of the methyl azide → methanimine rearrangement are visualized on the hypersurface cut (Figure 5), generated by selecting the coordinates  $d_{\text{N}^1\text{N}^2}$  and  $\angle\text{H}^1\text{CN}^1$  to represent the altogether  $3 \times 7 - 6 = 15$  degrees of freedom of the seven-atom system. In addition, the MNDO-optimized geometries are given for methylnitrene and all saddle points, i.e. for asynchronous N<sub>2</sub> splitoff followed by 1,2 H shift (Figure 5A:  $\Delta\text{O}\Delta\Rightarrow$ ) as well as for the synchronous movement of (N<sup>2</sup>N) and H<sup>1</sup> (Figure 5S:  $\bullet\blacktriangle\Rightarrow$ ) to yield methanimine. Before the hypersurface is discussed in more detail (Figure 5), its approximate character<sup>10</sup> based on the semiempirical MNDO procedure<sup>48</sup> without explicit consideration of electron correlation has to be pointed out. However, the heuristic experience is that experimental observations especially for organic nitrogen compounds are usually reproduced by the results of MNDO calculations.<sup>2,3,10,48b</sup>

**Asynchronous N<sub>2</sub> extrusion** to yield the singlet methylnitrene in its lowest  $\bar{A}(^1\text{E})$  state, calculated to be endothermic by 190 kJ/mol (eq 11), can be described to a first approximation with a one-dimensional "reaction driver" coordinate (Figure 5A): Starting from the known structure of methyl azide,<sup>49</sup> the distance H<sub>3</sub>CN<sup>1</sup>-N<sup>2</sup>N is increased in 10-pm steps, and the remaining bond distances and angles are optimized by the respective MNDO subroutine.<sup>48</sup> Predicted are an activation energy of ~220 kJ/mol and a more productlike transition state with an N<sup>1</sup>...N<sup>2</sup> distance of ~200 pm. Systematic saddle-point search via gradient norm

minimization yields 217 kJ/mol and 202 pm, respectively. The subsequent 1,2 H shift starting from one of the rather shallow  $\bar{A}(^1\text{E})$  Jahn-Teller minima of methylnitrene (Figure 5:  $\circ$ ) is calculated to be strongly exothermic (Figure 5:  $\Delta H_f^{\text{MNDO}} = -390$  kJ/mol). The rearrangement of the five-atom species H<sub>3</sub>CN possessing  $3 \times 5 - 6 = 9$  degrees of freedom can be visualized on the very same hypersurface because the distance N<sup>1</sup>...N<sup>2</sup> is too long to cause any substantial perturbation. The activation barrier amounts to only ~20 kJ/mol and the C-N<sup>1</sup> bond length remains approximately constant. As concerns the individual movements, once the three-membered ring saddle point has been reached (Figure 5:  $\blacktriangle$ ), first the H<sub>2</sub>C group planarizes fully and then rotates. Summarizing, singlet methylnitrene, being located in a rather shallow minimum, should easily tautomerize even at low temperatures as has been proven by matrix experiments.<sup>5f,23,27,28</sup>

**Synchronous N<sub>2</sub> splitoff with 1,2 H shift** (Figure 5S), as expected, proceeds via a three-membered ring saddle point at a less elongated N<sup>1</sup>...N<sup>2</sup> distance. A stroboscopic representation of the individual movements along the reaction path of minimum total energy, accomplished by simultaneous plotting of equidistant structures along the reaction coordinate (Figure 6), shows that the CN distance shortens while N<sup>1</sup>...N<sup>2</sup> widens, that the H<sub>2</sub>C group is almost planarized before it rotates, and that the changing angle  $\angle\text{CN}^1\text{N}^2$  is responsible for the curved trajectory of the leaving N<sub>2</sub> molecule.

When we return to the MNDO heat of formation hypersurface, obviously—within the error limit of the semiempirical approach neglecting electron correlation as well as molecular dynamics—for both asynchronous and synchronous methyl azide decomposition activation barriers of comparable size are estimated (Figure 5:  $\Delta\Delta H_f^{\text{MNDO}} \leq 60$  kJ/mol).

The MNDO hypersurface calculations have been extended to also cover the gas-phase pyrolysis of ethyl, isopropyl, and *tert*-butyl azides. Because the substituent dependence of their decomposition temperatures (cf. following section) suggests synchronous N<sub>2</sub>

(48) (a) Dewar, M. J. S.; Thiel, W. *J. Am. Chem. Soc.* **1977**, *99*, 4899.  
(b) *Ibid.* **1977**, *99*, 4907.

(49) Salathiel, W. F.; Curl, R. F., Jr. *J. Chem. Phys.* **1966**, *44*, 1288.

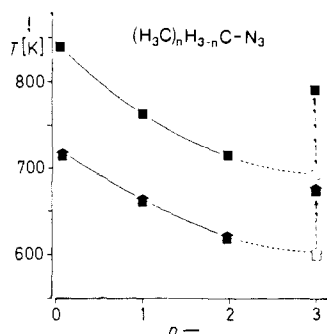


Figure 7. PE spectroscopically determined temperatures of beginning (●) and complete (▲) decomposition of alkyl azides  $(\text{H}_3\text{C})_n\text{H}_{3-n}\text{CN}_3$  ( $n = 1-3$ ); for the  $\text{H} \rightarrow \text{CH}_3$  extrapolation ( $\circ, \Delta$ ) see text.

elimination and 1,2 H shift or 1,2  $\text{CH}_3$  migration, only values for these processes are presented (Table I).

Inspection of the MNDO results (Table I) shows both the starting alkyl azides as well as the resulting methane imine derivatives to be stabilized by increasing alkyl substitution. The same applies to the energies of the respective saddle points. The gradient norm minimized structures closely resemble each other, e.g. exhibiting an  $\text{H}^1$ -bridged three-membered ring as well as a rather short  $\text{N}^1 \cdots \text{N}^2$  distance. For ethyl and isopropyl azides, 1,2 H shift is preferred over 1,2  $\text{CH}_3$  migration, with the saddle point for *tert*-butyl azide lying above the one for the hydrogen shift in the ethyl azide decomposition.

**Substituent Dependence of Alkyl Azide Decomposition Temperatures.** When we return once more to the approximate MNDO hypersurface (Figure 5), both principal decomposition pathways, i.e. the asynchronous one via a methylnitrene intermediate and the synchronous one with concerted  $\text{N}_2$  extrusion and 1,2 H shift, seemed feasible according to the energy barriers estimated within the expected error limits. Attempts to rationalize the PE spectroscopically determined temperatures for initial  $\text{N}_2$  extrusion (Figure 7: ●) and for complete azide decomposition (Figure 7: ▲) with increasing C-methylation, however, favor a synchronous process.

The temperatures for  $\text{RN}_3$  pyrolyses in eq 3, 6, 7, and 8 under constant and (nearly) unimolecular flow conditions are found within a relatively narrow range, e.g. for beginning  $\text{N}_2$  elimination between 620 K for isopropyl azide (eq 7) and 720 K for methyl azide (eq 3). Both curves for initial and complete  $\text{N}_2$  extrusion run parallel to each other, and an extrapolation of the temperature parabolas obtained for  $(\text{H}_3\text{C})_n\text{H}_{3-n}\text{CN}_3$  decomposition accompanied by 1,2 H shift ( $n = 0-2$ ) to *tert*-butyl azide ( $n = 3$ ) results in values (Figure 7: ○, Δ) approximately 70 K below those measured. This is in accord with numerous literature reports<sup>46</sup> that 1,2 alkyl migrations require higher activation energies than 1,2 H shifts.

The PE spectroscopically observed substituent dependence of the  $\text{RN}_3$  decomposition temperatures, which reflect the activation barriers for the rate-determining step, favors a synchronous process for the following reasons: Contrary to our pyrolysis results, photolysis experiments in which nitrenes are formed show the  $\text{RN}-\text{NN}$  bond breaking to be largely independent of the substituent  $\text{R}$ <sup>46</sup> and, therefore, an accompanying 1,2-migration of a hydrogen or a methyl group has to be assumed for the rate-determining step of the thermal  $\text{N}_2$  extrusion. Furthermore, both the experiments<sup>5,23,27</sup> as well as the calculations (cf. e.g. Figure 5) agree in a rather small barrier for the nitrene rearrangement relative to that for the initial  $\text{N}_2$  splitoff. In addition, using an approximate Arrhenius relationship (eq 12) to compare  $\text{N}_2$  elim-

$$k = A e^{-E/RT} = A' e^{-E'/RT'} = k' \quad (12)$$

$$\Delta E = [R \ln(A/A') + \Delta E/T] T' \sim T' \Delta E/T$$

ination temperatures  $T'$  (Figure 7: ●) of alkyl azides  $\text{RN}_3$  relative to the temperatures  $T$  for  $\text{H}_3\text{CN}_3$  to the calculated MNDO activation barriers<sup>3</sup>  $\Delta E'$  for the asynchronous  $\text{N}_2$  extrusion (Figure

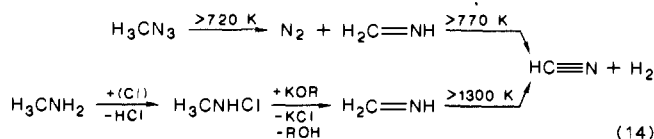
5A) or for the synchronous process (Figure 5S and Table I) relative to  $\Delta E$  for  $\text{H}_3\text{CN}_3$ , yields the ratios in eq 13.

	R = $\text{CH}_3$	$\text{CH}_2\text{CH}_3$	$\text{CH}(\text{CH}_3)_2$	$\text{C}(\text{CH}_3)_3$	
$T'/T$	1.00	0.92	0.86	0.93	
(A) $\Delta E'/\Delta E$	1.00	0.99	1.00	1.02	(13)
(S) $\Delta E'/\Delta E$	1.00	0.94	0.91	1.02	

Obviously, only the  $E'/\Delta E$  ratios for the synchronous pathway (eq 13S) parallel the experimentally determined temperature ratios for differently methylated azides. Therefore, the substituent dependence of the decomposition temperatures supports the assumption that alkyl azide pyrolysis proceeds along a synchronous path, i.e. with the  $\text{N}_2$  extrusion coupled to the 1,2 R shift (cf. Figures 5S and 6).

**Chemical Activation of Methanimine Intermediates.**<sup>2,3</sup> Under the constant conditions for low-pressure pyrolysis in the flow reactor (eq 5) used, methanimine intermediates could be detected PE spectroscopically only in the decomposition of alkyl,<sup>2,4</sup> allyl,<sup>2,42</sup> or vinyl<sup>28</sup> azides and of trimethylenetetrazole,<sup>2,3</sup> which on heating presumably first opens its tetrazole ring to the corresponding valence tautomeric azide. In contrast, none have been observed in the thermolyses of azides like  $\text{F}_2\text{HCN}_3$ ,<sup>2,13</sup>  $\text{ClH}_2\text{CCH}_2\text{N}_3$ ,<sup>2,14</sup>  $\text{F}_3\text{CN}_3$ ,<sup>2,15</sup>  $\text{NCH}_2\text{CN}_3$ ,<sup>2,3</sup> or  $\text{NCN}_3$ ,<sup>2,3</sup> which contain acceptor substituents and which in addition to the azide  $\text{N}_2$  are capable of splitting off other thermodynamically favorable leaving groups like HF, HCl, HCN, or  $\text{N}_2$ .

In general, products of exothermic gas-phase reactions may be formed considerably chemically activated, whereas in solution the reaction enthalpy stored as vibratory, rotatory, and translatory energy in the resulting molecules usually is quickly dissipated by frequent collisions.<sup>47,50</sup> In the vapor phase, particularly at low pressure, the collision frequency drops drastically and the heat of the reaction contained in the respective products can induce consecutive processes. Chemical activation<sup>47,50</sup> becomes even more obvious, if the very same compound prepared in different ways is thermally decomposed to an identical product under otherwise comparable conditions. For the reaction of methanimines,  $\text{R}_2\text{C}=\text{NR} \rightarrow \text{RC}\equiv\text{N} + \text{RR}$ , to alkanenitriles, considerable temperature differences are observed depending on whether the gas stream from azide pyrolysis is heated further (cf. eq 2, 3, and 6-8)—for instance, in a second oven inserted in (eq 5)<sup>2,8</sup>—or whether the "cold" imine, condensed in a cooling trap, is re-evaporated and thermally decomposed. A particularly drastic temperature difference has been observed for the parent methanimine either generated by methyl azide pyrolysis (eq 3) or prepared by the heterogeneous chlorination of methylamine over *N*-chlorosuccinimide and subsequent dehydrochlorination of the *N*-chloromethylamine over solid potassium *tert*-butylate (cf. the Experimental Section)<sup>2,33</sup> (eq 14). The temperature difference,



determined PE spectroscopically by the appearance of the HCN ionization pattern between 13.6 and 14.2 eV (cf. Figure 1), amounts to over 500 K(!).<sup>2,3,33b</sup> To quote an additional example, the rearrangement of 2*H*-azirine to acetonitrile also requires a temperature higher by 120 K than that necessary for its formation in the pyrolysis of vinyl azide (eq 2).

For the unimolecular thermal decomposition of methyl azide, one estimates on the basis of literature bond enthalpy data and on the activation barrier for  $\text{N}_2$  extrusion that the resulting  $\text{H}_2\text{C}=\text{NH}$  molecule might be chemically activated by approximately 340 kJ/mol (Figure 8).<sup>2,47</sup>

In satisfactory agreement, MNDO calculations predict an  $\text{N}_2$  extrusion activation energy of about 220 kJ/mol and, for the

(50) Cf. e.g. the review on unimolecular dynamics in: Hase, H. L. *Potential Energy Surfaces and Dynamics Calculations*; Truhlar, D. G., Ed.; Plenum: New York, 1981; p 1 ff, and literature cited therein.



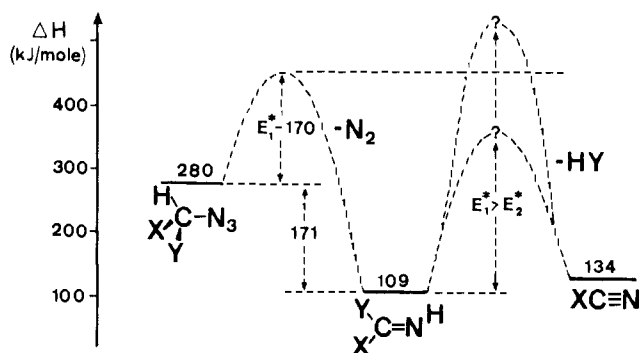


**Figure 8.** Enthalpy diagram for the thermal decomposition of azides  $XYHCN_3$  in consecutive reaction channels via methanimine intermediates  $XYC=NH$  to the nitriles  $XC\equiv N$ . Values given refer to X, Y = H (see text).

strongly exothermic  $H_2C=NH$  formation, a reaction enthalpy of 170 kJ/mol.<sup>3</sup> Since the "excess" energy stored in the molecule cannot be "dissipated" under the nearly unimolecular conditions in the low-pressure gas stream (Figure 1), already a small increase in temperature leads to the elimination of  $H_2$  and formation of HCN (Figure 8: X, Y = H). In contrast, the thermal dehydrogenation of isolated methanimine requires that the full activation energy (Figure 8:  $E_2^*$ ) be supplied, i.e. a temperature higher by more than 500 K.

According to the PE spectroscopic observations, the chemically activated imine intermediates formed in alkyl azide pyrolyses can eliminate not only  $H_2$  (cf. eq 3 and 6) but also  $CH_4$  (cf. eq 6 and 7),  $H_3CCH_3$  (cf. eq 7 and 8), or  $H_2C=CH_2$  (eq 9) to form nitriles in an entropy-controlled reaction. According to the enthalpy diagram (Figure 8), all azides  $(HYX)CN_3$  for which the second activation barrier  $E_2^*$  is relatively low should split off a further molecule fragment HY together with  $N_2$ . The experimental result that in gas-phase pyrolyses of acceptor-substituted azides<sup>2,13-15</sup> the corresponding imines, in spite of their demonstrated stability, are not observed PE spectroscopically is thus readily explained: The  $N_2$  extrusion from e.g.  $F_2CHN_3$ <sup>13</sup> or  $ClCH_2CH_2N_3$ ,<sup>14</sup> which only commences at relatively high temperatures, leads to the intramolecular explosion of the chemically activated imine intermediate. The considerable reaction enthalpies, which are stored in the molecular fragment remaining after  $N_2$  extrusion, also help to answer questions as to why, for example, phenylsilyl triazide  $H_5C_6Si(N_3)_3$  in its 1000 K gas-phase pyrolysis "suddenly" splits off four molecules of  $N_2$  and why the moiety  $H_5C_6SiN$  left over

can rearrange to the thermodynamically more stable isomer phenyl silaisocyanide  $H_5C_6N\equiv Si$  (eq 1).

### Conclusions

Gas-phase pyrolysis of alkyl azides, i.e. compounds that tend to explode violently when ignited in condensed phase, can be studied without much risk in low-pressure flow systems using PE spectroscopic real-time analysis. Information gathered comprises detection and subsequent isolation of methanimine intermediates, which in a consecutive reaction channel split off  $H_2$ , alkanes, or alkenes to form alkanenitriles. Accompanying MNDO calculations prove valuable not only in the assignment of ionization patterns and thus in the identification of decomposition products at various temperatures but also in providing some insight into the complex microscopic path of the alkyl azide pyrolysis. According to both the experiments and the calculations, supplemented by preceding literature reports, the  $N_2$  extrusion under unimolecular conditions requires unexpectedly high temperatures and proceeds in a synchronous way to yield singlet  $N_2$  and, via 1,2 H or 1,2  $CH_3$  shifts, the respective methanimines. These intermediates are formed chemically activated because the considerable reaction enthalpy of the exothermic  $N_2$  extrusion cannot be dissipated by collisions under unimolecular conditions and may even lead to their "thermal explosion" splitting off additional fragments.

It is hoped that the demonstrated safe handling of the treacherous alkyl azides in the gas phase will be of interest to other research groups with access to measurement techniques of higher time resolution than photoelectron spectroscopy. Especially, a more detailed investigation of the chemically activated methanimine intermediates may improve the presently still fragmentary knowledge concerning the microscopic reaction pathways of medium-sized molecules.

**Acknowledgment.** The research project has been generously supported by the Deutsche Forschungsgemeinschaft within the special program "short-lived molecules", by the Fonds der Chemischen Industrie, and by the Federal State of Hesse. R.D. thanks the Studienstiftung des Deutschen Volkes for a stipend.

**Registry No.**  $H_3CNHCl$ , 6154-14-9;  $CH_3CN$ , 75-05-8;  $CH_3CH=NH$ , 20729-41-3;  $(CH_3)_2C=NCH_3$ , 6407-34-7;  $H_3CCH_3$ , 74-84-0; HCN, 74-90-8; *cis*- $H_3CCH=NH$ , 56003-82-8; *trans*- $H_3CCH=NH$ , 56003-81-7;  $(CH_3)_2C=NH$ , 38697-07-3;  $H_2C=NCH_3$ , 1761-67-7; *cis*- $H_3CCH=NCH_3$ , 64611-40-1; *trans*- $H_3CCH=NCH_3$ , 19885-67-7; methyl azide, 624-90-8; ethyl azide, 871-31-8; isopropyl azide, 691-57-6; *tert*-butyl azide, 13686-33-4; allyl azide, 821-13-6; allyl azide dimer, 36895-17-7; methanimine, 2053-29-4; dimethyl sulfate, 77-78-1; diethyl sulfate, 64-67-5; isopropyl bromide, 75-26-3; *tert*-butyl chloride, 507-20-0; allyl iodide, 556-56-9; methylamine, 74-89-5.